

# Sparse Bayesian Lasso via a Variable-Coefficient $\ell_1$ Penalty

Nathan Wycoff<sup>1</sup>, Ali Arab<sup>2</sup>, Katharine M. Donato<sup>3,4</sup>, Lisa O. Singh<sup>1,5</sup>

<sup>1</sup> The McCourt School's Massive Data Institute, Georgetown University

<sup>2</sup> Department of Mathematics and Statistics, Georgetown University

<sup>3</sup> The Institute for the Study of International Migration, Georgetown University

<sup>4</sup> The School of Foreign Service, Georgetown University

<sup>5</sup> Department of Computer Science, Georgetown University

November 10, 2022

## Abstract

Modern statistical learning algorithms are capable of amazing flexibility, but struggle with interpretability. One possible solution is *sparsity*: making inference such that many of the parameters are estimated as being identically 0, which may be imposed through the use of nonsmooth penalties such as the  $\ell_1$  penalty. However, the  $\ell_1$  penalty introduces significant bias when high sparsity is desired. In this article, we retain the  $\ell_1$  penalty, but define learnable penalty weights  $\lambda_p$  endowed with hyperpriors. We start the article by investigating the optimization problem this poses, developing a proximal operator associated with the  $\ell_1$  norm. We then study the theoretical properties of this variable-coefficient  $\ell_1$  penalty in the context of penalized likelihood. Next, we investigate application of this penalty to Variational Bayes, developing a model we call the Sparse Bayesian Lasso which allows for behavior qualitatively like Lasso regression to be applied to arbitrary variational models. In simulation studies, this gives us the Uncertainty Quantification and low bias properties of simulation-based approaches with an order of magnitude less computation. Finally, we apply our methodology to a Bayesian lagged spatiotemporal regression model of internal displacement that occurred during the Iraqi Civil War of 2013-2017.

*Keywords:* variational Bayesian inference, sparsity, proximal operators, nonsmooth optimization, gravity model, human migration

# 1 Introduction

**Basic Inferential Problem:** Sparsifying penalties are popular because they allow for simultaneous variable selection and parameter estimation by shrinking parameter values identically to 0. Explicitly, we define the sparse learning problem as follows:

$$\min_{\boldsymbol{\beta}, \boldsymbol{\theta}} \mathcal{L}(\boldsymbol{\beta}, \boldsymbol{\theta}) + \tau \|\boldsymbol{\beta}\|_0, \quad (1)$$

where  $\boldsymbol{\beta}$  is a parameter vector which we wish to be sparse,  $\boldsymbol{\theta}$  is a vector of other model parameters and  $\mathcal{L}$  is a term which determines the compatibility of a parameter configuration with a dataset (such as a log-likelihood or log posterior density). This is a difficult problem because the  $\|\cdot\|_0$  function, which counts the nonzero components of its input, is nonconvex and discontinuous. The  $\|\cdot\|_1$  norm is a useful approximation because it is the closest convex function to  $\|\cdot\|_0$ . This is the penalty function of the celebrated Lasso (Tibshirani, 1996; Taylor et al., 1979), which may be viewed as placing a Laplace prior on  $\beta_p$  (Park and Casella, 2008). The draw-back to this convexity is bias: estimates of nonzero parameters will be shrunk towards zero, significantly so if we are to achieve much sparsity (Zhang, 2010). One solution to this problem is to allow the penalty coefficients to vary by parameter:

$$\min_{\boldsymbol{\beta}, \boldsymbol{\theta}} \mathcal{L}(\boldsymbol{\beta}, \boldsymbol{\theta}) + \tau \sum_{p=1}^P \lambda_p |\beta_p|, \quad (2)$$

as when  $\lambda_p \rightarrow 0$  the associated  $\beta_p$  is unpenalized. Far from clear is how to choose these  $\lambda_p$ , as evidenced by the assortment of approaches discussed in the next section.

**Existing Approaches and Limitations:** The importance of variable selection in non-linear models has prompted decades of research and yielded a multitude of approaches. In this section, we review selected penalty-based approaches to variable selection.

Some approaches perform adaptation “offline”, that is, before or after the optimization process. The Adaptive Lasso (Zou, 2006) specifies  $\lambda_p = \frac{1}{|\hat{\beta}_p|^\gamma}$ , where  $\hat{\beta}_p$  is some initial

estimate of the regression coefficient and  $\gamma$  is a hyperparameter, though an initial estimate  $\hat{\beta}_p$  is a nontrivial task if  $\mathcal{L}$  is complicated. Bühlmann and Meier (2008); Candès et al. (2008) propose to iterate this procedure, updating the penalty coefficient  $\lambda_p$  with new  $\hat{\beta}_p$ . Alternatively, we may adopt a two-stage process, using Lasso for variable selection only and proceeding to an unpenalized procedure (Efron et al., 2004; Meinshausen, 2007; Zou and Li, 2008).

Several authors have proposed simulation-based procedures for adaptation of  $\lambda_p$ . Kang and Guo (2009); Leng et al. (2014); Mallick and Yi (2014) place a Gamma prior or similar for  $\lambda_p$  and conduct inference via Gibbs sampling. Bhattacharya et al. (2012) instead take the approach of specifying a Dirichlet prior on the regression coefficients before conducting MCMC. Conceptually this is similar to the Horseshoe Prior (Carvalho et al., 2010), which instead specifies a conditional Normal prior for  $\beta_p$ . The Horseshoe prior enjoys generality as well as fast specific implementations (Terenin et al., 2019; Makalic and Schmidt, 2015). The reader is referred to Bhadra et al. (2019) for an extensive comparison of the Lasso and Horseshoe models. Another approach is the Spike-Slab prior (Mitchell and Beauchamp, 1988) which uses discrete latent variables to categorize whether  $\beta_p$  was *a priori* sampled from the spike or the slab, which would complicate gradient-based inference.

Variational Bayesian inference (Blei et al., 2017, VB) is another way to adapt the  $\lambda_p$ . But there is a sense in which VB with a Laplace prior differs from Lasso: the integrated cost erases the sparsifying geometry, as we discuss. Previous work has circumvented this using either a point mass variational distribution for regression coefficients (Tung et al., 2019), which does not directly allow for uncertainty quantification (without, say, bootstrapping Fu and Knight (2000)), or by thresholding small coefficients (Babacan et al., 2014), which requires setting an arbitrary threshold (She, 2009). Kawano et al. (2015) vary the threshold

while monitoring information criteria.

Nonconvex penalties do not vary the regularization strength but are directly constructed to impose minimal bias on nonzero coefficients, such as the Smoothly Clipped Absolute Deviation function (Fan and Li, 2001; Hunter and Li, 2005, SCAD) or Minimax Concave Penalty (Zhang, 2010, MCP). These penalties do not correspond to proper priors, as they place constant, positive probability density arbitrarily far from the origin.

Other penalties, like the ridge penalty (Hoerl and Kennard, 1970) and elastic net (Zou and Hastie, 2005), do not serve primarily to select variables, but rather to stabilize model fit or improve predictions. These are not the subject of this article.

**Scientific Motivation:** Forced human migration is at an all time high and only increasing. In order for policymakers to plan effectively, it is important to understand which factors affect when and where people will move during times of crisis. Traditionally, migration researchers use *gravity models*, described in Section 4.1.2. These models were developed by economist to model international trade (the flow of goods and services) as a function of traditional econometric indicators, typically on a coarse spatiotemporal scale (i.e. country by year). Migration researchers use this model because it can be effective in capturing both push and pull dynamics. In this article, we study an approximately year-long period of the Iraqi Civil War of 2013-2017, where the government and its international backers fought ISIL (Islamic State, also known as ISIS) in the northeast of the country. Traditional migration variables are not immediately available in exactly those situations where they are needed most: dangerous, remote, and underdeveloped areas, such as our case study. Taking advantage of the proliferation of the mobile internet, we develop novel social media “Buzz Variables” derived from Arabic-Language twitter (Section 4.1.1). This allows us to make predictions at finer spatiotemporal scales than traditional country-year level admin-

istrative data, but introduces new challenges, namely unignorable lag between cause and effect, spatiotemporal correlation, and high dimensional and noisy predictors. In order to meet these new challenges, we develop a Bayesian hierarchical model which allows for zero inflation, overdispersion, spatiotemporal random effects, and lagging and aggregation of predictors (Section 4.2) – a complex model to perform variable selection on.

**Brief Outline of Our Contributions:** We begin this article with a study of the approach of treating the Laplace inverse scale parameter  $\boldsymbol{\lambda} := \{\lambda_1, \dots, \lambda_P\}$  as an additional parameter to be optimized, one endowed with the hyperprior  $p_\lambda$ , which yields the following optimization:

$$\min_{\beta, \theta, \boldsymbol{\lambda} > \mathbf{0}} \mathcal{L}(\beta, \theta) + \sum_{p=1}^P [\tau \lambda_p |\beta_p| + \log \lambda_p] + \sum_{p=1}^P -\log p_\lambda(\lambda_p), \quad (3)$$

where  $\tau$  is a positive parameter controlling the sparsity level and the  $\log \lambda_p$  term comes from the normalization constant of the Laplace density. The  $\ell_1$  penalty in general may be efficiently applied to a smooth loss function via the Iterative Shrinkage and Thresholding Algorithm (Daubechies et al., 2004, ISTA), a proximal gradient method Parikh et al. (2014). But ISTA assumes a known and fixed  $\lambda_p$ . Section 2 examines a proximal operator associated with the variable- $\lambda_p$  optimization problem and discusses how to deploy it to marry adaptive and nonsmooth penalties in an analog of ISTA we term Variable ISTA (VISTA)<sup>1</sup>. It also investigates the basic theoretical properties of this procedure in penalized likelihood.

In Section 3 we pivot to a Variational Bayesian take on an adaptive Lasso using a nonsmooth penalty we term the Sparse Bayesian Lasso (SBL). The “Bayesian Lasso” of Park and Casella (2008) is so named as it is a Bayesian explanation for the density used in Lasso. But the Laplace prior does not actually encode the prior beliefs that motivate the use of Lasso, i.e., that the coefficient vector is sparse. Rather, it encodes the belief that most of

---

<sup>1</sup>As we deploy Nesterov acceleration, the better analog is actually Fast ISTA (Beck and Teboulle, 2009).

the coefficients are near zero, which leads to poor interval coverage and bias if they are not. As such it is not *operationally* a Bayesian Lasso, that is, it is not a method that yields the sparsity properties of Lasso as part of a Bayesian analysis. The proposed Sparse Bayesian Lasso fills this role by allowing for both geometric sparsity and uncertainty quantification. Combined with warm starts<sup>2</sup>, we can efficiently calculate trajectories not just of parameter estimates, as in the traditional Lasso, but of entire variational distributions, showing us how uncertainty of model parameters change with sparsity. This allows us to avoid specifying or estimating an overall model complexity parameter  $\tau$ , which is difficult in practice.

Most practitioners using bespoke statistical models do so in a software environment that makes inference straightforward to conduct given a model specification. In this article, we explain how to deploy our method in gradient-based learning frameworks such as `tensorflow` and `pytorch`. After verifying the frequentist properties of the SBL in simulation studies, we demonstrate the potential of the SBL in complex hierarchical models using our Iraq forced displacement case study (Section 4). We conclude by discussing research directions suggested by the novel proximal operator in Section 5.

## 2 Coefficient-Specific $\lambda_p$ with Optimization

We begin this section by developing a proximal gradient method suitable for general smooth optimization problems augmented by the variable-coefficient  $\ell_1$  penalty. We then describe basic theoretical properties of the estimator in the penalized likelihood case. We simply give outlines of proofs for theoretical results; detailed derivations are available in the Supplementary Material.

---

<sup>2</sup>A “warm start” is simply the practice of initializing an iterative algorithm at the final step of a previous, similar algorithm.

## 2.1 Background: Nonsmooth Penalties and Proximal Operators

We are interested in minimizing a complicated but smooth loss  $l$  augmented with a simple but nonsmooth regularizer  $g$ :

$$c(\mathbf{x}) = l(\mathbf{x}) + \lambda g(\mathbf{x}), \quad (4)$$

where  $g$  is given by the  $\ell_1$  norm in the case of Lasso regression. Proximal gradient descent and its relatives are the algorithms of choice in such a situation. Given a function  $g$  with domain  $\mathcal{X}$  and some norm parameterized by a positive definite matrix  $\mathbf{C}$ , their *proximal operator* is then defined as the following mapping:

$$\text{prox}_g^{\mathbf{C}}(\mathbf{x}) = \underset{\mathbf{u} \in \mathcal{X}}{\text{argmin}} g(\mathbf{u}) + \frac{1}{2} \|\mathbf{x} - \mathbf{u}\|_{\mathbf{C}}^2. \quad (5)$$

Intuitively, the proximal operator of a function  $g$  evaluated at a vector  $\mathbf{x}$  returns another vector  $\mathbf{u}$  which is close to  $\mathbf{x}$  (wrt  $\mathbf{C}$ ) but does a better job minimizing  $g$ .

Proximal Gradient algorithms optimize the objective function in Equation 4 via iteration of a two step process. Given a current solution  $\mathbf{x}^k$  and smooth cost function  $\mathcal{L}$ , the next iterate is parameterized by a step size  $s$  and given by:

$$\hat{\mathbf{x}}^{k+1} = \mathbf{x}^k - s\mathbf{C}^{-1}\nabla\mathcal{L}(\mathbf{x}^k) \quad (6)$$

$$\mathbf{x}^{k+1} = \text{prox}_g^{s\mathbf{C}}(\hat{\mathbf{x}}^{k+1}). \quad (7)$$

Note that  $\mathbf{C}$  is scaled by the step size in the proximal operator and that we have not included a subgradient of  $g$  in the gradient descent step. The matrix  $\mathbf{C}$  may in theory be any positive definite matrix and in practice it is defined by the preconditioning strategy of the gradient descent algorithm that the proximal operator will be deployed in.

The proximal operator is most useful when it can be computed efficiently. In this article, we will assume a diagonal preconditioner  $\mathbf{C} = \text{diag}(c_1, \dots, c_P)$ , which is conducive

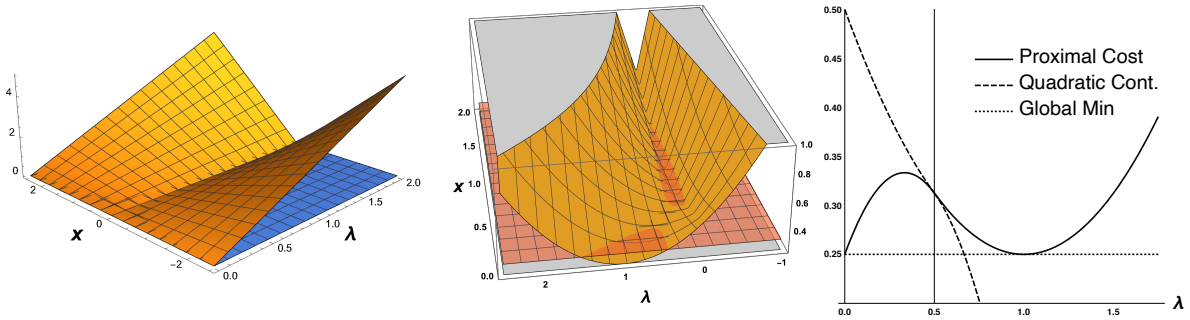


Figure 1: **The Proximal Cost** *Left:* The function  $g(x, \lambda) = \lambda|x|$ . The proximal cost *Center:* of  $(x, \lambda)$  *Right:* marginal for  $\lambda$  with  $\lambda_0 = x_0 = 1$ ;  $s_\lambda = s_x = 2$  yielding two optima.

to breaking the proximal problem into subproblems defined along each axis. For example, when  $g : \mathbb{R} \rightarrow \mathbb{R}$  is given by  $g(x) = \lambda|x|$ , the proximal operator is given by elementwise application of the Soft Thresholding Operator (STO):

$$[\text{prox}_{\lambda, |}^{\text{sdiag}(c_1, \dots, c_p)}(\mathbf{x})]_p = (|x_p| - s_{c_p} \lambda)^+ \text{sgn}(x_p), \quad (8)$$

where  $(a)^+$  gives  $\max(0, a)$  and  $\text{sgn}(a)$  gives the sign of  $a$ .

## 2.2 The Variable-Coefficient $\ell_1$ Proximal Operator

Because the  $\ell_1$  regularization coefficient  $\lambda$  is now being optimized over, the STO is no longer the pertinent proximal operator. Indeed, the  $\ell_1$  regularization function, considered formally as a function of both  $\lambda$  and  $\mathbf{x}$ , is nonconvex (see Figure 1, Left), somewhat complicating proximal operator computation. In fact, many authors such as Parikh et al. (2014) define the prox operator as one that acts on convex functions. However, there has been work on extending proximality to larger classes of functions (see e.g. (Hare and Sagastizábal, 2009)) and, of particular interest to the statistical community, development of proximal operators for the nonconvex “Bridge Penalties”  $|\beta_p|^q$  for  $q \in (0, 1)$  (Marjanovic and Solo, 2013); see Polson et al. (2015) for more on proximal methods in statistics. Perhaps because of this focus on convexity (and despite the popularity of the  $\ell_1$  norm and adaptive

penalty methods), the proximal operator of  $\lambda|x|$  as a  $\mathbb{R}^+ \times \mathbb{R} \rightarrow \mathbb{R}^+$  function has not to our knowledge been previously examined in the literature. It turns out that the action  $\text{prox}(\mathbf{x}, \boldsymbol{\lambda})$  of this proximal operator is available in closed form. It is single-valued for almost all inputs and always for sufficiently small step sizes  $s_x$  and  $s_\lambda$  such that  $s_x s_\lambda < 1$ .

Consider the proximal operator of the variable-coefficient  $\ell_1$  norm function  $g(\mathbf{x}, \boldsymbol{\lambda}) = \sum_{p=1}^P \lambda_p |x_p|$ . Since this function decomposes into additive functions of each  $(\lambda_p, x_p)$  individually, its proximal operator acts on each block independently of the others. Therefore, for the remainder of this section, we consider a single block  $(\lambda, x)$ , dropping the index  $p$ , and consider the proximal operator of the 2-dimensional function  $g(x, \lambda) = \lambda|x|$ :

$$\text{prox}_g^{s_\lambda, s_x}(x_0, \lambda_0) = \underset{x \in \mathbb{R}, \lambda > 0}{\text{argmin}} \lambda|x| + \frac{(x - x_0)^2}{2s_x} + \frac{(\lambda - \lambda_0)^2}{2s_\lambda}. \quad (\text{P1})$$

**Lemma 1.** *The marginal cost of P1 with respect to  $\lambda$  (i.e. with  $x$  profiled out) is the following piecewise quadratic expression:*

$$\underset{\lambda > 0}{\text{argmin}} \begin{cases} \frac{1}{2} \left( \frac{1}{s_\lambda} - s_x \right) \lambda^2 + (|x_0| - \frac{\lambda_0}{s_\lambda}) \lambda + \frac{\lambda_0^2}{2s_\lambda} & \lambda < \frac{|x_0|}{s_x} \\ \frac{(\lambda - \lambda_0)^2}{2s_\lambda} + \frac{x_0^2}{2s_x} & \lambda \geq \frac{|x_0|}{s_x} \end{cases}, \quad (9)$$

where the changepoint  $\lambda = \frac{|x_0|}{s_x}$  is the point where  $\lambda$  is just large enough to push  $x$  to zero.

*Proof.* Convert to nested optimization and exploit the known solution for fixed  $\lambda$  given by the soft thresholding operator. □

The quadratic polynomial in the interval  $[\frac{|x_0|}{s_x}, \infty]$  is always convex. When  $s_\lambda s_x < 1$ , the quadratic polynomial in the other interval is convex as is the overall expression. But when  $s_\lambda s_x > 1$ , the coefficient of the quadratic term is negative, and that polynomial is concave, yielding a nonconvex piecewise function (see Figure 1, center and right).

We are now prepared to develop the proximal operator.

**Theorem 1.** *The optimizing  $\lambda$  for the proximal program P1 is given by, when  $s_x s_\lambda < 1$ :*

$$\lambda^* = \begin{cases} \lambda_0 & \lambda_0 \geq \frac{|x_0|}{s_x} \\ \frac{(\lambda_0 - s_\lambda |x_0|)^+}{1 - s_\lambda s_x} & o.w. \end{cases}, \quad (10)$$

and, when  $s_x s_\lambda \geq 1$ , by  $\lambda^* = \mathbb{1}_{\left[\frac{\lambda_0}{\sqrt{s_\lambda}} > \frac{|x_0|}{\sqrt{s_x}}\right]} \lambda_0$  (here  $\mathbb{1}$  denotes the indicator function). In either case  $x^* = (|x_0| - s_x \lambda^*)^+ \text{sgn}(x_0)$ .

*Proof.* We need only compare the optima of the quadratic functions of Lemma 1. □

**Remark 1.** *Due to the nonconvexity of the proximal cost, this proximal program may have two global optima. Thus the proximal operator is discontinuous and multi-valued at the discontinuity, as visualized in the top right of Figure 2.*

**Remark 2.** *When  $s_x s_\lambda < 0$  and  $\lambda_0 < s_\lambda |x_0|$  or when  $s_x s_\lambda > 1$  and  $\frac{\lambda_0}{\sqrt{s_\lambda}} > \frac{|x_0|}{\sqrt{s_x}}$ , the solution to the proximal problem gives  $\lambda = 0$ , which would lead to no shrinkage on  $\beta$ .*

Remark 2 is interesting, as it implies that it is possible to develop a procedure with “dual sparsity”: on the regression coefficient, when appropriate, or on the penalty coefficient. However, in our application of this operator to the Laplace penalty, the  $\lambda$  normalization term gives this a density of zero, precluding that point being a penalized maximizer. We look forward to examining other models which allow for zero penalties.

This proximal operator has been conceptualized as a mapping of  $(\lambda_0, x_0) \rightarrow (\lambda^*, x^*)$  parameterized by  $s_x$  and  $s_\lambda$ , but to visualize it we will briefly study it as a function of these four quantities mapping to an optimizing  $\lambda^*$ .

**Remark 3.** *Since when  $s_x s_\lambda > 1$  the  $\lambda^*$  is either 0 or  $\lambda_0$ , we will focus on the case where  $s_x s_\lambda < 1$ . Then, let  $a := \frac{|x_0|}{s_x}$  and  $b := s_x s_\lambda$ . We can rewrite the solution as a function of*

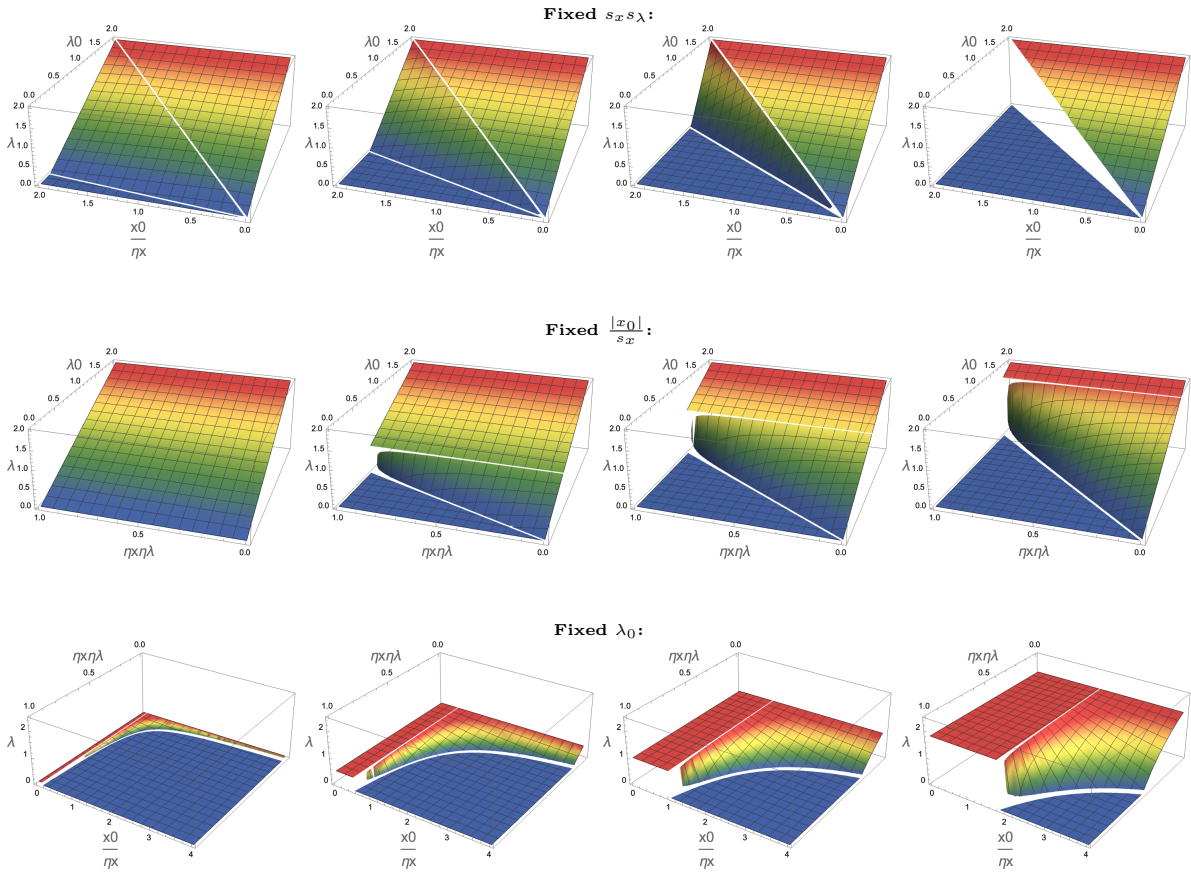


Figure 2: **The Action of the Proximal Operator:** Plots of the reduced proximal operator (Eq 11) considering two variables at a time and fixing the third. *Top:* for various fixed  $b := s_x s_\lambda < 1$  and with  $\lambda_0, \frac{|x_0|}{s_x} \in (0, 2)$ . Values  $b = s_x s_\lambda \in \{0.1, 0.35, 0.65, 0.99\}$  are shown left to right. *Mid:*  $a = \frac{|x_0|}{s_x} \in \{0, 0.5, 1, 1.8\}$ . *Bottom:*  $\lambda_0 \in \{0.2, 0.75, 1.25, 1.75\}$ .

*just three variables:*

$$\lambda(\lambda_0, a, b) = \begin{cases} \lambda_0 & \lambda_0 \geq a \\ \frac{(\lambda_0 - ab)^+}{1 - b} & o.w. \end{cases} \quad (11)$$

This function is visualized in Figure 2. For given step size product  $b$  the function is stepwise linear, and converges to the identity mapping with respect to its  $\lambda_0$  input as  $b \rightarrow 0$ . As  $b \rightarrow 1$ , the mapping becomes more and more steep for  $\lambda_0 \in (ab, a)$ , gradually converging to the discontinuous mapping  $\lambda(\lambda_0, a, b) \rightarrow \lambda_0 \mathbb{1}_{\lambda_0 > a}$ . The proximal operator is

multi-valued at  $\lambda_0 = a$  when  $b = 1$ .

**Comparison to Other Penalties in Statistics:** Existing nonconvex alternatives to our proposed biconvex penalty in the form of the MCP, SCAD and Bridge penalties all come with an extra hyperparameter controlling how close the penalty gets to approximating  $\|\cdot\|_0$  directly. One advantage of the biconvex penalty proposed here is that it does retain only the single global penalty strength parameter, which in practice means it is possible to simply try the model at all pertinent parameter values via a sequence of warm starts, which significantly speed up the optimization. However, it does require specification of a prior on  $\lambda$ . While this can be a limitation for some applications, we have found the standard Half-Cauchy to be sufficient across ours. We wish also to note that it is easy to show that in the special case where  $P_\lambda$  is given by an exponential distribution with rate parameter  $\epsilon$ , our penalty is equivalent to the log-sum penalty of Candès et al. (2008). Viewed from this perspective, we see that there are potential gains to debiasing when a heavier-tailed prior is used on  $\lambda$ .

### 2.3 Deploying the prox operator with VISTA

We can deploy the proximal operator of Equation 10 as part of a basic proximal gradient method as follows:

$$\tilde{\beta}^{t+1} \leftarrow \beta^t - s_\beta \nabla_{\beta} \mathcal{L}(\beta^t, \lambda^t) \tag{12}$$

$$\tilde{\lambda}^{t+1} \leftarrow \lambda^t - s_\lambda \nabla_{\lambda} [\mathcal{L}(\beta^t, \lambda^t) - \log \lambda^t - \log P_\lambda(\lambda^t)] \tag{13}$$

$$\beta^{t+1}, \lambda^{t+1} \leftarrow \text{prox}_g^{s_\lambda, s_\beta}(\tilde{\beta}^{t+1}, \tilde{\lambda}^{t+1}) \tag{14}$$

In practice, success with any gradient descent method relies on choosing good step sizes, preconditioners, and acceleration. We discuss the details of our optimization procedure in Supplementary 1.

## 2.4 Basic Theoretical Properties for Penalized Likelihood

In this section, we will assume that  $\lambda$  is excluded from the misfit term  $\mathcal{L}(\beta)$  such that it only appears in the penalty and its hyperprior. In this case, we can rewrite our penalty as such (we will assume all parameters are penalized for ease of discussion; this does not constrain the generality of the following results):

$$\min_{\beta, \lambda > 0} \mathcal{L}(\beta) + \sum_{p=1}^P [\tau \lambda_p |\beta_p| + \log \lambda_p] + \sum_{p=1}^P -\log p_\lambda(\lambda_p) \quad (15)$$

$$\iff \min_{\beta} \mathcal{L}(\beta) + \sum_{p=1}^P \min_{\lambda > 0} [\tau \lambda_p |\beta_p| + \log \lambda_p - \log p_\lambda(\lambda_p)] \quad (16)$$

Therefore, we may profile over  $\lambda$  to develop a penalty  $g_\tau(|\beta|) = \min_{\lambda > 0} \tau \lambda |\beta| + \log \lambda + \rho(\lambda)$ , where  $\rho(\lambda) = -\log p_\lambda(\lambda)$ . We will use the notation  $\lambda_a$  for the optimizing  $\lambda$  at  $\theta = 0$ , which satisfies  $\lambda_a = \frac{1}{\rho'(\lambda_a)}$ . We begin with some basic properties of this penalty.

**Lemma 2.** *The following hold, where  $\lambda^*$  denotes the optimizing  $\lambda$ , and is formally a function of  $\tau$  and  $|\beta|$ :*

1.  $\lambda^* = \frac{1}{\tau |\beta| + \rho'(\lambda^*)}$ .
2.  $\frac{\partial \lambda^*}{\partial |\beta|} = -\frac{\tau}{\lambda^{*2} + \rho''(\lambda)}$ .
3.  $g'_{\tau_n}(|\beta|) = \tau \lambda^*$ .
4.  $\lim_{|\beta| \rightarrow 0} p'_{\tau_n}(|\beta|) = \frac{\tau}{\rho'(\lambda_a)}$ .

*Proof.* These follow from implicit differentiation on first order optimality conditions.  $\square$

This allows us to quantify the behavior of this penalty as follows:

**Theorem 2.** *Assume that the logarithmic derivative of the hyperprior density on  $\lambda$  is bounded ( $|\rho'(\lambda)| < M_1 \forall \lambda \geq 0$ ) and that the density is decreasing on  $(0, \infty)$ . Then:*

1.  $g'_\tau(|\beta|) \approx \frac{1}{|\beta|}$  for large  $\beta$ .
2. The minimum of  $|\beta| + g'_\tau(|\beta|)$  is achieved at  $\beta = 0$  with value  $\lambda_a \tau$ .

*Proof.* Follows from Lemma 2. □

**Remark 4.** *Fan and Li (2001) describe three desirable properties of nonconcave penalties: first, that they have bias decreasing quickly in nonzero parameter size, second, that they induce sparsity, and third, that they be continuous in the data. The shrinking gradient size with parameter norm is sufficient to ensure unbiasedness for large parameters. The fact that the minimum of  $|\beta| + g'_\tau(|\beta|)$  is strictly positive ensures sparsity, while the fact that the minimum occurs at zero ensures continuity. This latter condition is not satisfied by, for example, the bridge penalty.*

**Remark 5.** *Bounded logarithmic derivatives are satisfied by the densities of, for example, the Cauchy and Exponential distributions, but not the Gaussian distribution.*

Let us now consider the penalized linear regression case, and develop the limiting distribution of the estimator  $\hat{\beta}_n = \min_{\beta} \sum_{i=1}^N (y_i - \mathbf{x}_i^\top \beta) + \sum_{p=1}^P \min_{\lambda > 0} [\tau_n \lambda_p |\beta_p| + \log \lambda_p - \log p_\lambda(\lambda_p)]$  under the assumption of error terms  $\epsilon_i \sim \mathcal{N}(0, \sigma^2)$ . Following Fu and Knight (2000); Zou (2006), we define the following random function which  $\hat{\beta}$  is a transformed minimum of:

$$V_n(\mathbf{u}) = \sum_{i=1}^N \left[ \left( \epsilon_i - \frac{\mathbf{u}^\top \mathbf{x}_i}{\sqrt{n}} \right)^2 - \epsilon^2 \right] + \sum_{p=1}^P g_{\tau_n}(|\beta_p + \frac{u_p}{\sqrt{n}}|) - g_{\tau_n}(|\beta_p|) \quad (17)$$

**Theorem 3.** *Let  $\tau_n = \sqrt{n}\tau_0$ ,  $\mathbf{C} := \lim_{n \rightarrow \infty} \frac{1}{n} \mathbf{X}_n^\top \mathbf{X}_n$ , and  $\mathbf{w} \sim \mathcal{N}(0, \sigma^2 \mathbf{C})$ ,  $|\rho'(\lambda)| \leq M_1$ . Then:*

$$\sqrt{n}(\hat{\beta}_n - \beta) \xrightarrow{d} \operatorname{argmin}(V)$$

with

$$V(\mathbf{u}) = -2\mathbf{u}^\top \mathbf{w} + \mathbf{u}^\top \mathbf{C} \mathbf{u} + \sum_{p=1}^P g_{\tau_0}(\mathbf{u}) \mathbb{1}_{\{\beta_p=0\}}$$

*Proof.* Follows from the fact that  $\frac{dg_{\tau_n}(|\beta|)}{d|\beta|}$  shrinks for large arguments and from the singularity of  $g_{\tau_n}(|\beta|)$  at the origin. □

The fact that the penalty term does not appear in the limiting optimization problem when the true coefficient is nonzero suggests that we can, as Fu and Knight (2000) noted, expect convergence of our estimators at the usual rate without asymptotic bias while simultaneously shrinking unimportant parameters exactly to zero in finite samples.

### 3 The Sparse Bayesian Adaptive Lasso

Having developed a general-purpose optimization algorithm and developed basic properties in the penalized likelihood case, we pivot to developing a Bayesian Lasso procedure which provides full uncertainty quantification and penalty coefficient adaptation. We achieve this by deploying the VISTA procedure of the previous section on a novel nonsmooth Variational Bayesian methodology which we call the Sparse Bayesian Adaptive Lasso.

#### 3.1 Variational Inference and Nonsmooth Penalties

Variational Bayes searches for a distribution over an unknown parameter vector  $\boldsymbol{\theta}$  that is 1) analytically tractable, and 2) sufficiently close to the posterior such that what each has to say about the quantities of interest are approximately the same. It does so by defining an optimization problem  $\operatorname{argmin}_{Q_\theta \in \mathcal{Q}} d(Q_\theta, P_{\theta|\mathbf{y}})$  where  $P_{\theta|\mathbf{y}}$  is our true posterior probability with density  $p$  and  $Q_\theta$  is a candidate variational distribution with density  $q$  from a space of possible distributions  $\mathcal{Q}$  parameterized by *variational parameters*, and  $d$  is some measure of dissimilarity between distributions. In this article, for each parameter  $\theta$ , the variational distribution is defined by a location parameter  $\eta_\theta$  and a scale parameter  $\nu_\theta$ . We will impose variational independence as is common:  $q_{\boldsymbol{\eta}, \boldsymbol{\nu}}(\boldsymbol{\theta}) = \prod_{m=1}^M q_{\eta_m, \nu_m}(\theta_m)$ .

The most common  $d$  is the KL divergence from variational to posterior:

$$d(Q, P) = \text{KL}(Q_\theta || P_{\theta|\mathbf{y}}) = \mathbb{E}_{\theta \sim Q} \left[ \log \left( \frac{q(\boldsymbol{\theta})}{p(\boldsymbol{\theta}|\mathbf{y})} \right) \right] = -\mathbb{E}_{\theta \sim Q} [\log \mathcal{L}(\mathbf{y}|\boldsymbol{\theta})] + \text{KL}(Q_\theta || P_\theta). \quad (18)$$

We see this  $d(Q_\theta, P_{\theta|\mathbf{y}})$  may be viewed as the negative expected log likelihood (which we can view as a model misfit term) penalized by the KL divergence between the variational and prior distributions (which we can view as a model complexity term). Since  $Q$  was chosen to be simple, we can use a Monte Carlo sample to estimate the expected likelihood.

For the regression coefficients  $\beta_p$ , we specify Laplace distributions both for variational and prior distributions:  $\beta_p \stackrel{Q}{\sim} \text{L}(\eta_{\beta_p}, \nu_{\beta_p})$  and  $\beta_p \stackrel{P}{\sim} \text{L}(0, \frac{1}{\lambda_p \tau})$ , leading to the following penalty function on our variational parameters  $\eta_{\beta_p}$  and  $\nu_{\beta_p}$ :

$$g_{\text{KL}}(\eta_{\beta_p}, \nu_{\beta_p}, \lambda_p) = \text{KL}(\text{L}(\eta_{\beta_p}, \nu_{\beta_p}) || \text{L}(0, \frac{1}{\lambda_p \tau})) = \tau \lambda (\nu_{\beta_p} e^{-\frac{|\eta_{\beta_p}|}{\nu_{\beta_p}}} + |\eta_{\beta_p}|) - \log(\nu_{\beta_p}) - \log \lambda. \quad (19)$$

One might be forgiven for thinking that Variational Bayes, a procedure built on optimization, would be the approach that allows us to combine the generality afforded by Bayesian inference with the sparsity of penalized likelihood procedures. Unfortunately, this is not the case. The proof of this is straightforward, but we have not seen it explicitly mentioned in the academic literature.

**Theorem 4.** *Penalty functions defined by KL-cost Variational Bayesian procedures with continuous prior and variational distributions do not induce sparsity.*

*Proof.* As Fan and Li (2001, Section 2) discuss in the context of penalized likelihood, any penalty function which induces sparsity and is continuous in the data must have a singularity at the origin. Since Variational Bayesian penalties are defined by a prior-variational KL divergence, and this in turn is defined by an integral, an application of the fundamental theorem of calculus is sufficient to reach the desired conclusion.  $\square$

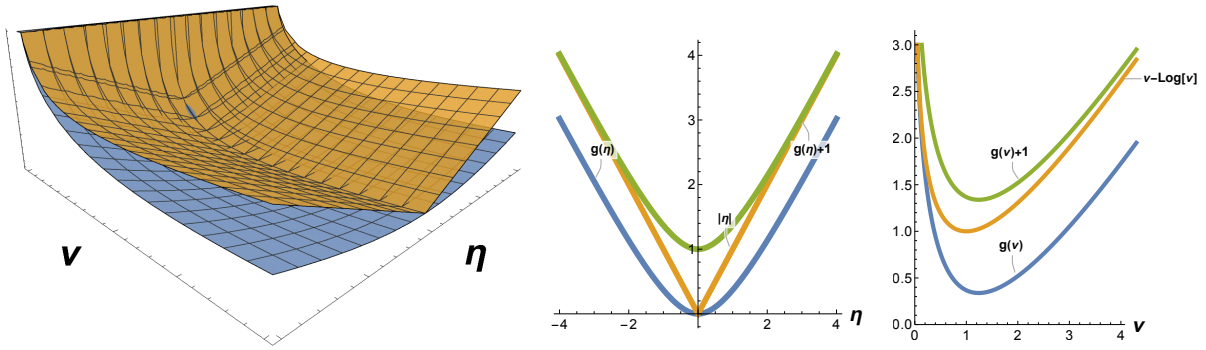


Figure 3: **Nonsmooth Approximation** *Left*: Bivariate KL penalty (blue) and nonsmooth approximation (orange). The marginal penalties, ( $g$  gives KL) for *Center*:  $\eta$ , *Right*:  $\nu$ .

The penalty given in Equation 19 is smooth despite the two absolute values because they cancel at zero as visualized in Figure 3 and demonstrated algebraically by Meyer (2021), who studied this function because of its similarity to the Huber loss function.

### 3.2 A Nonsmooth Approximation

Owen (2007), in the context of penalized M estimation, advocates to reintroduce nonsmoothness by exchanging the quadratic and linear parts of the penalty. We propose to approximate  $\nu_{\beta_p} e^{-\frac{|\eta_{\beta_p}|}{\nu_{\beta_p}}} + |\eta_{\beta_p}|$  by  $\nu_{\beta_p} + |\eta_{\beta_p}|$  since it is a good approximation for small  $\nu_{\beta_p}$ :

$$g_{\text{NS}}(\eta_{\beta_p}, \nu_{\beta_p}, \lambda_p) := \tau \lambda_p (\nu_{\beta_p} + |\eta_{\beta_p}|) - \log(\nu_{\beta_p}) - \log \lambda_p - 1. \quad (20)$$

Figure 3 show that  $g_{\text{NS}}$  retains the qualitative properties of the KL penalty, and  $g_{\text{NS}}(\eta_{\beta_p}, \nu_{\beta_p}) - 1$  bounds  $g_{\text{KL}}(\eta_{\beta_p}, \nu_{\beta_p})$  from below. Notice that the term  $\log \eta_{\beta_p}$  serves as a logarithmic barrier preventing  $\eta_{\beta_p} \rightarrow 0$ . Therefore, the sparsity induced by this penalty is qualitatively different from that induced by the Horseshoe, or Spike-Slab, which compress the entire posterior distribution to zero. In contrast, this proposed penalty sets only the variational mode exactly to zero while allowing for nonzero, and sometimes significant, variational variance.

In the case of a linear regression with Gaussian error, the cost is closed form whenever the first two moments of  $Q_{\beta}$  and the inverse and log expectation of  $Q_{\sigma^2}$  are tractable (Supplementary 2). We cannot expect this to be the case in general, and must estimate the expected log likelihood term  $-\mathbb{E}_{\theta \sim Q_{\theta}}[\log \mathcal{L}(\mathbf{y}|\theta)]$ . Most common in “blackbox” VB (Ranganath et al., 2014) is to optimize this with stochastic optimization over a Monte Carlo sample. We instead use the Sample Average Approximation (Robinson, 1996, SAA), which converts the optimization to a deterministic one by employing the same Monte Carlo draw throughout the optimization procedure, and use antithetic sampling for variance reduction (Owen, 2013, Chapter 8.2). Collecting those parameters which are not desired to be sparse into the vector  $\theta$  with associated variational parameters  $\eta_{\theta}, \nu_{\theta}$ , our cost is given as:

$$\min_{\eta} \frac{1}{B} \sum_{\theta_b \sim Q_{\theta}, \beta_b \sim Q_{\beta}} \mathcal{L}(\theta_b, \beta_b) + \sum_{p=1}^P g_{\text{NS}}(\eta_{\beta_{b,p}}, \nu_{\beta_{b,p}}, \lambda_p) + \text{KL}(Q_{\beta, \theta} || P_{\beta, \theta}) \quad (21)$$

Note that to compute gradients we must differentiate through the sampling procedure; this is generally implemented in automatic differentiation packages like `tensorflow` and `pytorch`, though quality of the gradients vary. When the distribution is a location-scale family, this differentiation is particularly straightforward (Kingma and Welling, 2014). With the gradient of the smooth part computed, we can apply the VISTA algorithm to yield sparse learning with any likelihood. Since  $\lambda_p$  is of secondary interest, we estimate it via maximization rather than specifying a distribution for it.

### 3.3 Building Coefficient Trajectories by Varying $\tau$

A practically useful aspect of Lasso regression is the ability to efficiently form trajectories of parameter estimates while varying the penalty strength  $\tau$  by warm-starting optimizations. We also deploy VISTA estimating the SBL with Gaussian error structure and a Half-Cauchy prior, illustrated in Figure 4, evaluate a trajectory for varying  $\tau$ , and then compare to the

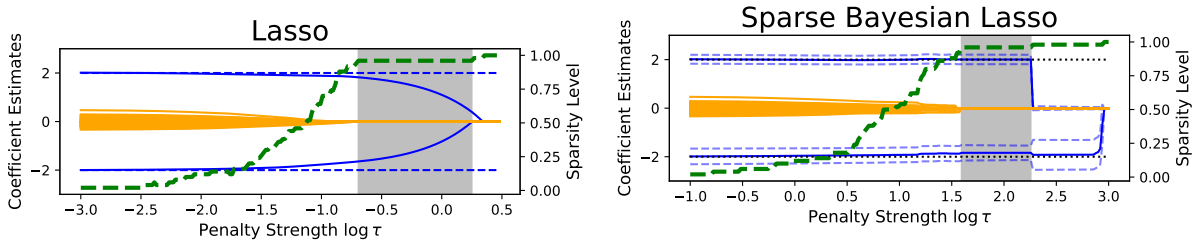


Figure 4: **Qualitative Behavior:** Solid lines indicate coefficient estimates (y-axis) as function of regularization strength for Lasso (left) SBL (right). Dotted blue lines give true nonzero coefficient values  $(-2,2)$ , and solid blue lines give estimates. Orange lines give estimates of coefficients which are 0. Dotted green line (second y-axis) gives percent of estimated coefficients estimated as 0 (sparsity).

Lasso on a simple simulated dataset with a true Gaussian-linear model in 50 dimensions. Though it successfully thresholds the active parameters last, there is no regularization strength which allows Lasso to identify the correct model without bias. In the SBL, by contrast, the active parameters are near their true values for the whole range of penalty values until they are thresholded out, closer to the behavior of nonconvex penalties such as MCP and SCAD.

### 3.4 Empirical Frequentist Properties

In this section, we examine the empirical performance of our proposed method on selected GLMs. We use the mean function described in our working example. We deploy the VISTA algorithm, implemented in `tensorflow_probability`, on for both MAP and VB inference with Bernoulli, Negative Binomial, Normal, and Poisson likelihoods using the canonical link functions and with the Cauchy likelihood with an identity link. We tuned sparsity level  $\tau$  by hand which is what we advocate doing in practice by examining the entire trajectory produced by varying  $\tau$  (Supplementary 4). We use a Monte Carlo sample size of 40. As a

Likelihood	Method	$\beta$ -FNR	$\beta$ -FPR	$\beta$ -coverage	$\sigma^2$ -coverage	Time (s)
bernoulli	VISTA-MAP	0.03	0.00	-	-	4.43
	VISTA-SBL	0.00	0.00	0.91	1.00	31.58
	Horseshoe	0.00	0.04	0.93	1.00	400.09
cauchy	SSLasso	0.88	0.00	-	-	0.02
	VISTA-MAP	0.30	0.00	-	-	6.43
	VISTA-SBL	0.00	0.03	0.94	0.97	40.86
nb	Horseshoe	0.00	0.00	0.94	0.87	458.67
	VISTA-MAP	0.00	0.02	-	-	6.31
	VISTA-SBL	0.00	0.00	0.95	1.00	28.77
normal	Horseshoe	0.00	0.00	0.94	1.00	962.86
	SSLasso	0.00	0.00	-	-	0.02
	VISTA-MAP	0.00	0.02	-	-	7.12
poisson	VISTA-SBL	0.00	0.00	0.94	1.00	34.93
	Horseshoe	0.00	0.00	0.95	1.00	39.10
	VISTA-MAP	0.00	0.00	-	-	18.01
poisson	VISTA-SBL	0.00	0.00	0.80	1.00	46.77
	Horseshoe	0.00	0.00	0.98	1.00	394.34

Table 1: FNR is False Negative Rate, FPR is False Positive Rater, COVR is 95% empirical interval coverage, time is elapsed real time in seconds for given  $\tau$ .

comparator, we show a **JAGS** implementation of the Horseshoe prior, run for 1,000 iterations after adaptation on two chains, which should represent a lower bound on the amount of computation required for inference in practice. Additionally, we compare to the Spike-Slab Lasso using the R package **SSLASSO** when the link function is the identity, namely on the Gaussian and Cauchy cases. The Spike-Slab Lasso penalty could of course be combined with a non-Gaussian likelihood, but solving the marginal problem for coordinate descent will no longer in general be in closed form and is not implemented in **SSLASSO**. In contrast, the proximal operator is the same for any differentiable likelihood.

As Table 1 shows, SBL is able to maintain high interval coverage using generally about an order of magnitude the elapsed real time of the Horseshoe prior. On the Negative Binomial likelihood, which is the likelihood we use in the case study of Section 4.3, we observe about a  $30\times$  speedup. The SSLasso is fast but not yet applicable to non-Gaussian likelihoods (estimation with Cauchy data goes poorly), and not able to provide UQ. The

performance gap is smaller on the Normal likelihood where the Gibbs sampler enjoys conjugacy.

## 4 Modeling Migration in Iraq

We begin this section with an overview of the classical Gravity Model. We then pivot to discussing the data set we collected, and finally present the results of our analysis.

### 4.1 ISIL and the 2013-2017 Iraqi Civil War

In late 2013, tensions between Sunni and Shia Muslims in the Anbar province of Iraq boiled over into violence between the Shia government and its allies against the Islamic State. The violence led to significant internal displacement which is the subject of our case study. In the absence of traditional migration variables, we consider the use of social media for capturing indirect indicators of migrations. Specifically, we focus on novel conversation buzz and insecurity predictors based on Twitter data.

#### 4.1.1 Data Collection and Processing

**Social Media Indicators** We collected Arabic language tweets between March 2016 and June 2017 from Twitter’s Streaming Application Program Interface (API). Buzz variables were formed by monitoring counts of keywords selected by Arabic language experts related to various migration-relevant topics, such as ethnic angst and discussion about the economy. We also formed sentiment indicators. Variables such as Social buzz for different demographic groups, (e.g. `Social-shia_buzz`), Insecurity, (e.g. `Insecurity-emotions`), Environmental (e.g. `Environmental-weather`) are examples of the 68 variables identified.

**Movement Data** We use the flow data provided by the International Organization for

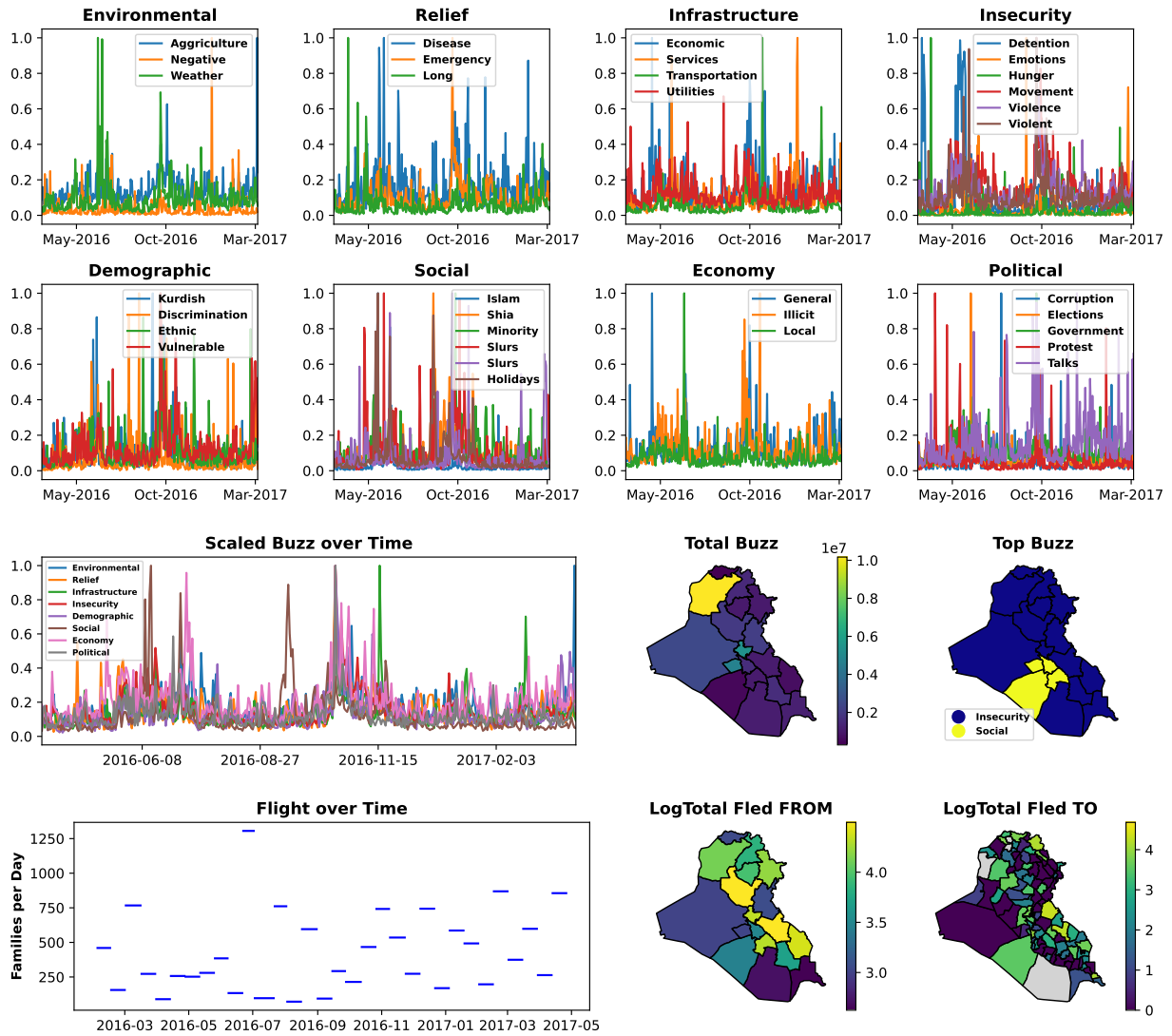


Figure 5: **Iraq Dataset:** *Top Two Rows:* Buzz Variables broken up by category and normalized to have max value 1. *Bottom Left Quadrant:* The cumulative buzz by each category is shown above the UN IOM data giving the families fleeing during each period. *Bottom Right Quadrant:* Spatial totals for Buzz (upper row) and flow (lower row); gray districts not observed.

Migration’s Iraq Displacement Tracking Matrix, which gives stocks of displaced families in one of 97 Districts, as well as which of the 18 Governorates they originated from. We differenced these data with respect to time to estimate flows. The counts are aggregated over variable length periods, with the shortest period consisting of 11 days and longest of 31 days. There are 48 total time periods in our study, leading to a total of 57,024 observations. 96.4% of response values are zero, with a mean of 6.71 families displaced for all time across origin-destination pairs.

#### 4.1.2 New Challenges for the Gravity Model

Gravity models of migration (Poprawe, 2015; Karemera et al., 2000; Ramos and Suriñach, 2017) measure the exchange between the origin  $o$  and destination  $d$  for a given time period  $t$ , denoted as  $y_{t,o,d}$ ; in our case study  $y_{t,o,d}$  is measured in number of families. The gravity model specifies a generalized linear model relating  $\mathbf{y} \in \mathbb{R}^{N_o N_d T}$  to predictors  $\mathbf{X} \in \mathbb{R}^{N_o N_d T \times P}$  as well as *resistance to exchange* terms  $\omega_t, \omega_o, \omega_d$  which represent the effects associated with each time periods, origin and destination. Poisson gravity models have been fit using MCMC for hospital patient flows (Congdon, 2000) and trade (Ranjan and Tobias, 2007). Chen et al. (2018) perform explicit Bayesian Model Selection on a gravity model of trade via Normal approximations to their likelihood. The fine timescale of our data introduces temporal misalignment between cause and effect: if an event which causes migration is recorded by our Twitter Buzz variables on a given day, we do not expect migrants to register at a camp the same day. At the yearly scale which gravity models are typically deployed, this is not a concern, but we need to develop a mechanism for estimating lags in this specific case study.

## 4.2 Spatiotemporal ZINB Gravity Model with Gaussian Lags

In this section, we develop the following hierarchical Bayesian model to relate the organic variables to the observed migration:

$$\lambda_p \stackrel{\text{iid}}{\sim} \text{C}(0, 1)^+ \text{ for } p \in \{1, \dots, P\} \quad (22)$$

$$\beta_p | \lambda_p \stackrel{\text{indep}}{\sim} \text{L}(0, \frac{1}{\tau \lambda_p})^+ \text{ for } p \in \{1, \dots, P\} \quad (23)$$

$$\phi_{\mathcal{I}} \sim \text{logitN}(a_\phi, b_\phi) \text{ for } \mathcal{I} \in \{\mathcal{T}, \mathcal{O}, \mathcal{D}\} \quad (24)$$

$$\rho_{\mathcal{I}}^2 \sim \text{logN}(a_\rho, b_\rho) \text{ for } \mathcal{I} \in \{\mathcal{T}, \mathcal{O}, \mathcal{D}\} \quad (25)$$

$$\boldsymbol{\omega}_{\mathcal{I}} | \phi_{\mathcal{I}}, \rho_{\mathcal{I}}^2 \sim \text{N}(\mathbf{0}, \rho_{\mathcal{I}}^2 \Sigma_{\mathcal{I}}(\phi_{\mathcal{I}})) \text{ for } \mathcal{I} \in \{\mathcal{T}, \mathcal{O}, \mathcal{D}\} \quad (26)$$

$$\pi \sim \text{logitN}(a_\pi, b_\pi) \quad (27)$$

$$y_{t,o,d} \sim \begin{cases} \delta_0 & \text{w.p. } \pi \\ \text{N.B.}(g(\mathbf{z}_{t,o,d}(\mu_l, \sigma_l)^\top \boldsymbol{\beta} + \omega_t + \omega_o + \omega_d), \frac{l_t}{\sigma^2})^3 & \text{o.w.} \end{cases} \quad (28)$$

where  $\phi_{\mathcal{T}} \in [0, 1]$  is the correlation between successive temporal fixed effects  $\boldsymbol{\omega}_t$  giving the AR1 correlation matrix  $\Sigma_t(\phi_t)$ , while  $\phi_o, \phi_d$  are the correlation parameters for the origin and destination spatial effects  $\boldsymbol{\omega}_{\mathcal{O}}, \boldsymbol{\omega}_{\mathcal{D}}$ , respectively, which are scaled to lie between the inverse maximum and minimum eigenvalues of the adjacency matrix (De Oliveira, 2012). These matrices are scaled by variance terms  $\rho_{\mathcal{I}}$  which are endowed with LogNormal priors. Given all these quantities, the number of families moving between two regions on a given day is given by a negative binomial distribution with success probability given by the canonical link transformation  $g$  of our linear predictions. The positive “number of failures” parameter controlling overdispersion is estimated by  $\frac{1}{\sigma^2}$  and is scaled by the duration of the time period  $l_t$ . Due to the preponderance of zeros in our model, we include the possibility of zero inflation by specifying a zero inflation parameter  $\pi$  with logitNormal prior. We account for unknown and variable lag between cause and effect through a “flattened” Gaussian filter

with parameter  $\mu_l$  determining how far back to shift the time series and the parameter  $\sigma_l$  determining how far outside the bounds of the period length to integrate (Supplementary 4 ). We use a neighborhood structure that has weight 1 if two regions touch and 0 otherwise.

#### 4.2.1 Variational Distribution and Inference

Parameters  $\lambda$ ,  $\beta$  and  $\sigma^2$  are estimated via the VISTA algorithm. We place logitNormal variational distributions on  $\phi_t, \phi_o, \phi_d, \pi$  and logNormal variational on  $\rho_t, \rho_o, \rho_d, \sigma^2$ . The KL divergence between prior and variational in all of these cases is given by the KL divergence of the underlying normal distributions and thus is available in closed form. The  $\omega$ 's are given a Normal variational distribution. While the KL divergence cannot completely be determined in closed form due to the spatiotemporal correlation parameters  $\phi$ , the  $\omega$  and  $\rho$  integrals may be computed analytically, and this expression may be evaluated for Monte Carlo samples of  $\phi$  without any matrix decompositions beyond an initial decomposition of the neighborhood structure matrix (Supplementary 4 ). As is done in the context of Gibbs sampling for CAR models, we “center on the fly” (Ferreira, 2019) by projecting the variational mean of  $\omega_{\mathcal{I}}$  to have mean 0 after each iteration:  $\eta_{\omega_{\mathcal{I}}} \leftarrow \eta_{\omega_{\mathcal{I}}} - \text{mean}(\eta_{\omega_{\mathcal{I}}})\mathbf{1}$ .

### 4.3 Results

In this section, we apply our methodology to our case study. We begin by setting the regularization coefficient  $\tau = 250$ , where the model chooses to include only the destination-level variable `insecurity-emotions-buz`. We then decreased this coefficient along a logarithmically spaced grid to  $\tau = 10$  with 100 points in between, plotting the trajectory of the variational distributions in Figure 6. Figure 6 shows the trajectory borne out by the regression coefficients, random effect variances and lag and zero inflation parameters. Begin

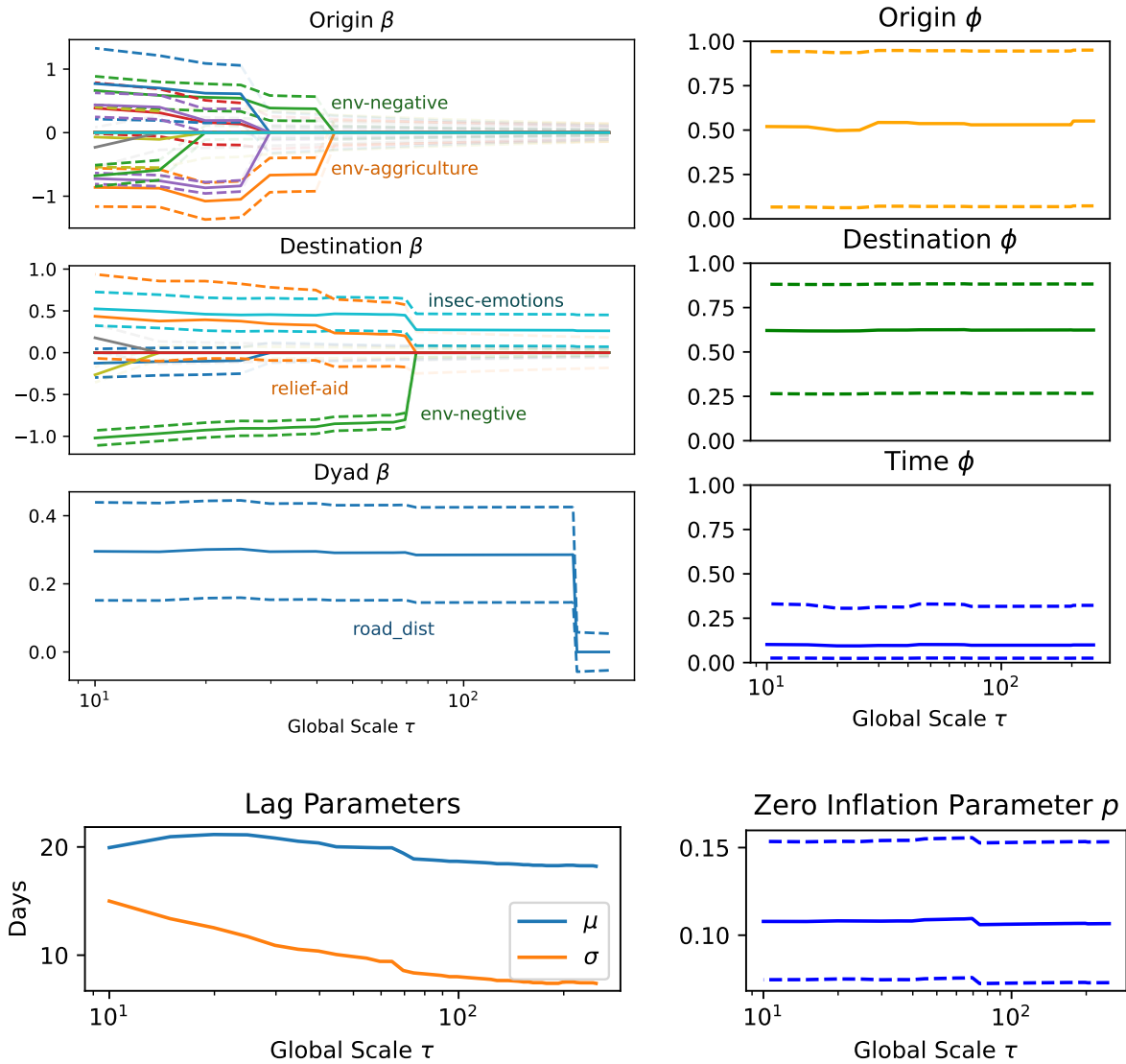


Figure 6: **Parameter Trajectories vs  $\tau$ .** *Top Left:* Regression Coefficient Variational Trajectory; dotted lines give 95% credible intervals; intervals are faded when the posterior mean is 0. *Top Right:* Spatiotemporal Correlations fairly constant. *Bottom Left:* Gaussian convolution parameters vary with fixed effects. *Bottom Right:* Zero inflation parameter is constant.

with the Left-Top three panels, which show the variational distributions of the regression coefficients. Qualitatively, we notice that variances of zeroed out coefficients decrease smoothly as the regularization strength increases, reflecting the increased prior distribution concentration. Nonzero coefficients, however, tend to have relatively stable values before experiencing jumps as new parameters enter. The first variable to enter the model is the `insecurity-emotions-buzz` variable associated with the destination. The next variable to enter is `road-dist`, the dyadic distance between origin and destination, which actually seems to indicate that migration occurs over longer distances (see Supplementary 4.4 for more discussion). The next variables to enter are again at the Destination level: `relief-aid` with a positive coefficient, indicating either that good relief aid attracts or is located where people are attracted, as well as `environment-negative` sentiment with a negative coefficient. The `environment-negative` sentiment at the Origin level is the next variable to enter, this time with the opposite coefficient, simultaneously with the `environment-agriculture` buzz at the Origin with a negative coefficient.

The lag-aggregation parameters are shown in the bottom left of Figure 6. We see that as the number of variables in the model increases, so too does the lookback window size  $\sigma_t$ , from about 9 days to about 15. The number of days to look back travels from around 18 to around 22. These results indicate that we can choose between a model with sharper predictions from fewer variables, or smoother predictions incorporating more variables and time. The spatiotemporal correlation parameters' variational distributions are shown in the top 3 right panels of Figure 6. The origin parameter is not well pinned down by our only 18 governorates, the Destination is also not strongly identified though it does rule out substantial negative spatial correlation, and the temporal correlation seems minimal. Finally, the bottom right panel indicates that the zero-inflation parameter is also fairly

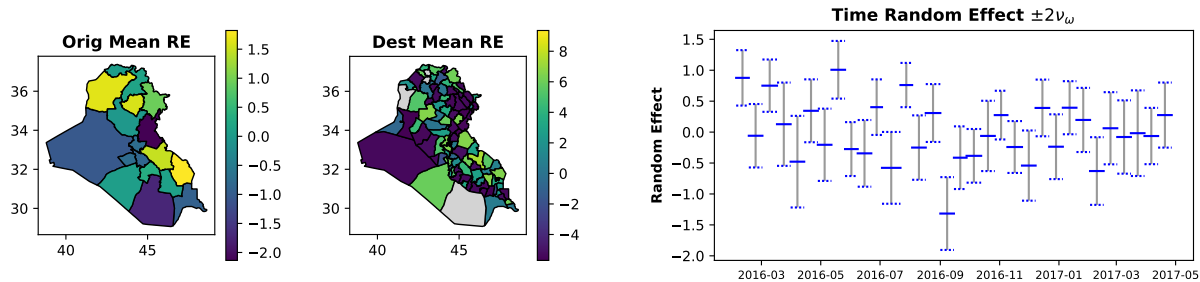


Figure 7: **Spatiotemporal Random Effects:** At the largest  $\tau$  value.

constant with respect to  $\tau$ , and somewhere between 8 and 15 percent. Recall that the data were over 95% zeros; most of these are being accounted for by the mean or correlation structure rather than the zero inflation.

One of the biggest and most positive origin random effects belongs to Ninewa Governorate, the capital of which is Mosul, a city which was the subject of fierce urban combat against ISIL. Maysan and Kirkuk governorates also large positive effects. The most negative effects belong to the Diyala Governorate, a Kurdish province in the East, and the Al-Muthanna Governorate, a southern province. For destinations, on the other hand, the Baghdad area has some of the highest effects, with its constituent Al-Sadr and Kut districts taking places one and two and fairly well separated from the rest. On the lower end we see a different story: many districts, most of which observed no inflow of migration, have random effects which are experiencing separation and have a value of about  $-5$ .

The time period with the largest random effect was from 2016-05-12 to 2016-05-26. According to a timeline from the Wilson Center (Center, 2019), this period saw a series of ISIL bomb attacks which left over 100 dead in Baghdad (May 12) as well as combat between Iraqi and ISIL forces. The period with the lowest random effect was 2016-09-01 to 2016-09-15, during which ISIL was more active abroad than in Iraq, also according to the Wilson Center’s timeline.

## 5 Discussion and Future Work

We began this article by examining the density of the Bayesian Lasso when  $\lambda_p$  is given a hyperprior and treated as a variable to optimize. This led to a biconvex proximal operator that is well defined for sufficiently small step sizes. We then showed how to plug this proximal operator into ISTA, producing the VISTA algorithm which allows for minimal bias even in the presence of high sparsity. Next, we examined the behavior of the MAP estimate in simple linear cases before developing a nonsmooth Variational Bayesian Lasso and deploying the VISTA algorithm on GLMs, where we found that our variational procedure had good frequentist coverage at less computational cost than simulation. Finally, we deployed the VISTA algorithm and Sparse Bayesian Lasso on a sophisticated hierarchical model and were able to generate trajectories of variational distributions of all model parameters, varying the penalty strength.

We look forward to deploying the VISTA algorithm on other applications such as the inverse and imaging problems where ISTA made its name. And we are even more excited to see what other possibilities viewing penalty coefficients as optimization quantities can open up. In particular, Group Lasso (Yuan and Lin, 2006) and Fused Lasso (Tibshirani et al., 2005), among other Lasso analogs, enjoy fast inference via proximal gradient methods as well; perhaps the variable-penalty versions of these proximal operators are available in closed form. Variable-coefficient low-rank penalties for matrices (e.g. Koltchinskii et al. (2011)) and their associated proximal operators are also of future interest. Recently, Quaini and Trojani (2022) developed basic inferential properties of estimators defined via a proximal operator; it would be interesting to see which of these properties apply to the biconvex proximal operator we have developed here. We are also curious about different ways to motivate nonsmoothness in VB, perhaps via different divergences or discontinuous priors.

## Acknowledgements

The authors gratefully acknowledge funding from the Massive Data Institute and McCourt Institute. We also acknowledge the Georgetown Data Lab and MDI Technical Team for support creating migration indices, and Douglas Post for his preliminary analysis of the Iraq data. We would like to thank Stephen Becker, Warren Hare, Nicholas Polson, Mahlet Tadesse, and Stefan Wild for valuable conversations and input. Any errors are our own.

## References

- Babacan, S. D., S. Nakajima, and M. N. Do (2014). Bayesian group-sparse modeling and variational inference. *IEEE transactions on signal processing* 62(11), 2906–2921.
- Beck, A. and M. Teboulle (2009). A fast iterative shrinkage-thresholding algorithm for linear inverse problems. *SIAM journal on imaging sciences* 2(1), 183–202.
- Bhadra, A., J. Datta, N. G. Polson, and B. Willard (2019). Lasso meets horseshoe: A survey. *Statistical Science* 34(3), 405–427.
- Bhattacharya, A., D. Pati, N. S. Pillai, and D. B. Dunson (2012). Bayesian shrinkage. *arXiv preprint arXiv:1212.6088*.
- Blei, D. M., A. Kucukelbir, and J. D. McAuliffe (2017). Variational inference: A review for statisticians. *Journal of the American statistical Association* 112(518), 859–877.
- Bühlmann, P. and L. Meier (2008). Discussion: One-step sparse estimates in nonconcave penalized likelihood models. *The Annals of Statistics* 36(4), 1534 – 1541.
- Candes, E. J., M. B. Wakin, and S. P. Boyd (2008). Enhancing sparsity by reweighted  $l_1$  minimization. *Journal of Fourier analysis and applications* 14(5), 877–905.

- Carvalho, C. M., N. G. Polson, and J. G. Scott (2010). The horseshoe estimator for sparse signals. *Biometrika* 97(2), 465–480.
- Center, W. (2019). Timeline: the rise, spread, and fall of the islamic state.
- Chen, H., A. Mirestean, and C. G. Tsangarides (2018). Bayesian model averaging for dynamic panels with an application to a trade gravity model. *Econometric Reviews* 37(7), 777–805.
- Congdon, P. (2000). A Bayesian approach to prediction using the gravity model, with an application to patient flow modeling. *Geographical analysis* 32(3), 205–224.
- Daubechies, I., M. Defrise, and C. De Mol (2004). An iterative thresholding algorithm for linear inverse problems with a sparsity constraint. *Communications on Pure and Applied Mathematics* 57(11), 1413–1457.
- De Oliveira, V. (2012). Bayesian analysis of conditional autoregressive models. *Annals of the Institute of Statistical Mathematics* 64(1), 107–133.
- Efron, B., T. Hastie, I. Johnstone, and R. Tibshirani (2004). Least angle regression. *The Annals of Statistics* 32(2), 407 – 499.
- Fan, J. and R. Li (2001). Variable selection via nonconcave penalized likelihood and its oracle properties. *Journal of the American Statistical Association* 96(456), 1348–1360.
- Ferreira, M. A. (2019). The limiting distribution of the Gibbs sampler for the intrinsic conditional autoregressive model. *Brazilian Journal of Probability and Statistics* 33(4), 734–744.
- Fu, W. and K. Knight (2000). Asymptotics for lasso-type estimators. *The Annals of statistics* 28(5), 1356–1378.

- Hare, W. and C. Sagastizábal (2009). Computing proximal points of nonconvex functions. *Mathematical Programming* 116(1), 221–258.
- Hoerl, A. E. and R. W. Kennard (1970). Ridge regression: Biased estimation for nonorthogonal problems. *Technometrics* 12(1), 55–67.
- Hunter, D. R. and R. Li (2005). Variable selection using MM algorithms. *The Annals of Statistics* 33(4), 1617 – 1642.
- Kang, J. and J. Guo (2009). Self-adaptive lasso and its Bayesian estimation. Technical report, Working Paper.
- Karemera, D., V. I. Oguledo, and B. Davis (2000). A gravity model analysis of international migration to north america. *Applied Economics* 32(13), 1745–1755.
- Kawano, S., I. Hoshina, K. Shimamura, and S. Konishi (2015). Predictive model selection criteria for Bayesian lasso regression. *Journal of the Japanese Society of Computational Statistics* 28(1), 67–82.
- Kingma, D. P. and M. Welling (2014). Auto-Encoding Variational Bayes. In *2nd International Conference on Learning Representations, ICLR 2014, Banff, AB, Canada, April 14-16, 2014, Conference Track Proceedings*.
- Koltchinskii, V., K. Lounici, and A. B. Tsybakov (2011). Nuclear-norm penalization and optimal rates for noisy low-rank matrix completion. *The Annals of Statistics* 39(5), 2302–2329.
- Leng, C., M.-N. Tran, and D. Nott (2014). Bayesian adaptive lasso. *Annals of the Institute of Statistical Mathematics* 66(2), 221–244.

- Makalic, E. and D. F. Schmidt (2015). A simple sampler for the horseshoe estimator. *IEEE Signal Processing Letters* 23(1), 179–182.
- Mallick, H. and N. Yi (2014). A new Bayesian lasso. *Statistics and its interface* 7(4), 571.
- Marjanovic, G. and V. Solo (2013). On exact l q denoising. In *2013 IEEE International Conference on Acoustics, Speech and Signal Processing*, pp. 6068–6072. IEEE.
- Meinshausen, N. (2007). Relaxed lasso. *Computational Statistics & Data Analysis* 52(1), 374–393.
- Meyer, G. P. (2021, jun). An alternative probabilistic interpretation of the huber loss. In *2021 IEEE/CVF Conference on Computer Vision and Pattern Recognition (CVPR)*, Los Alamitos, CA, USA, pp. 5257–5265. IEEE Computer Society.
- Mitchell, T. J. and J. J. Beauchamp (1988). Bayesian variable selection in linear regression. *Journal of the American Statistical Association* 83(404), 1023–1032.
- Owen, A. B. (2007). A robust hybrid of lasso and ridge regression. *Contemporary Mathematics* 443(7), 59–72.
- Owen, A. B. (2013). *Monte Carlo theory, methods and examples*.
- Parikh, N., S. Boyd, et al. (2014). Proximal algorithms. *Foundations and Trends in Optimization* 1(3), 127–239.
- Park, T. and G. Casella (2008). The Bayesian lasso. *Journal of the American Statistical Association* 103(482), 681–686.
- Polson, N. G., J. G. Scott, and B. T. Willard (2015). Proximal algorithms in statistics and machine learning. *Statistical Science* 30(4), 559–581.

- Poprawe, M. (2015, Jun). On the relationship between corruption and migration: empirical evidence from a gravity model of migration. *Public Choice* 163(3), 337–354.
- Quaini, A. and F. Trojani (2022). Proximal estimation and inference. *arXiv preprint arXiv:2205.13469*.
- Ramos, R. and J. Suriñach (2017). A gravity model of migration between the ENC and the EU. *Tijdschrift voor Economische en Sociale Geografie* 108(1), 21–35.
- Ranganath, R., S. Gerrish, and D. Blei (2014, 22–25 Apr). Black Box Variational Inference. In S. Kaski and J. Corander (Eds.), *Proceedings of the Seventeenth International Conference on Artificial Intelligence and Statistics*, Volume 33 of *Proceedings of Machine Learning Research*, Reykjavik, Iceland, pp. 814–822. PMLR.
- Ranjan, P. and J. L. Tobias (2007). Bayesian inference for the gravity model. *Journal of Applied Econometrics* 22(4), 817–838.
- Robinson, S. M. (1996). Analysis of sample-path optimization. *Mathematics of Operations Research* 21(3), 513–528.
- She, Y. (2009). Thresholding-based iterative selection procedures for model selection and shrinkage. *Electronic Journal of statistics* 3, 384–415.
- Taylor, H. L., S. C. Banks, and J. F. McCoy (1979). Deconvolution with the  $\ell_1$  norm. *Geophysics* 44(1), 39–52.
- Terenin, A., S. Dong, and D. Draper (2019). GPU-accelerated Gibbs sampling: a case study of the horseshoe probit model. *Statistics and Computing* 29(2), 301–310.
- Tibshirani, R. (1996). Regression shrinkage and selection via the lasso. *Journal of the Royal Statistical Society. Series B (Methodological)* 58(1), 267–288.

- Tibshirani, R., M. Saunders, S. Rosset, J. Zhu, and K. Knight (2005). Sparsity and smoothness via the fused lasso. *Journal of the Royal Statistical Society: Series B (Statistical Methodology)* 67(1), 91–108.
- Tung, D. T., M.-N. Tran, and T. M. Cuong (2019). Bayesian adaptive lasso with variational Bayes for variable selection in high-dimensional generalized linear mixed models. *Communications in Statistics-Simulation and Computation* 48(2), 530–543.
- Yuan, M. and Y. Lin (2006). Model selection and estimation in regression with grouped variables. *Journal of the Royal Statistical Society: Series B (Statistical Methodology)* 68(1), 49–67.
- Zhang, C.-H. (2010). Nearly unbiased variable selection under minimax concave penalty. *The Annals of Statistics* 38(2), 894 – 942.
- Zou, H. (2006). The adaptive lasso and its oracle properties. *Journal of the American statistical association* 101(476), 1418–1429.
- Zou, H. and T. Hastie (2005). Regularization and variable selection via the elastic net. *Journal of the royal statistical society: series B (statistical methodology)* 67(2), 301–320.
- Zou, H. and R. Li (2008). One-step sparse estimates in nonconcave penalized likelihood models. *The Annals of Statistics* 36(4), 1509 – 1533.

## SUPPLEMENTARY MATERIAL

**Python Package:** PyPI-package `sb1` containing code to perform the the methods outlined in this article.

**Supplementary Discussion and Results** PDF Document containing additional numerical results, mathematical details, and background.